

BGT24MTR11

Using BGT24MTR11 in Low Power  
Applications

24 GHz Radar

Application Note AN341

Revision: Rev. 1.0  
2013-12-02

**Edition 2013-12-02**

**Published by  
Infineon Technologies AG  
81726 Munich, Germany**

**© 2013 Infineon Technologies AG  
All Rights Reserved.**

#### **Legal Disclaimer**

The information given in this document shall in no event be regarded as a guarantee of conditions or characteristics. With respect to any examples or hints given herein, any typical values stated herein and/or any information regarding the application of the device, Infineon Technologies hereby disclaims any and all warranties and liabilities of any kind, including without limitation, warranties of non-infringement of intellectual property rights of any third party.

#### **Information**

For further information on technology, delivery terms and conditions and prices, please contact the nearest Infineon Technologies Office ([www.infineon.com](http://www.infineon.com)).

#### **Warnings**

Due to technical requirements, components may contain dangerous substances. For information on the types in question, please contact the nearest Infineon Technologies Office.

Infineon Technologies components may be used in life-support devices or systems only with the express written approval of Infineon Technologies, if a failure of such components can reasonably be expected to cause the failure of that life-support device or system or to affect the safety or effectiveness of that device or system. Life support devices or systems are intended to be implanted in the human body or to support and/or maintain and sustain and/or protect human life. If they fail, it is reasonable to assume that the health of the user or other persons may be endangered.

**Application Note AN341**

**Revision History: 2013-12-02**

**Previous Revision: prev. Rev.**

Page	Subjects (major changes since last revision)

**Trademarks of Infineon Technologies AG**

AURIX™, C166™, CanPAK™, CIPOS™, CIPURSE™, EconoPACK™, CoolMOS™, CoolSET™, CORECONTROL™, CROSSAVE™, DAVE™, DI-POL™, EasyPIM™, EconoBRIDGE™, EconoDUAL™, EconoPIM™, EconoPACK™, EiceDRIVER™, eupec™, FCOS™, HITFET™, HybridPACK™, I<sup>2</sup>RF™, ISOFACE™, IsoPACK™, MIPAQ™, ModSTACK™, my-d™, NovalithIC™, OptiMOS™, ORIGA™, POWERCODE™, PRIMARION™, PrimePACK™, PrimeSTACK™, PRO-SIL™, PROFET™, RASIC™, ReverSave™, SatRIC™, SIEGET™, SINDRION™, SIPMOS™, SmartLEWIS™, SOLID FLASH™, TEMPFET™, thinQ!™, TRENCHSTOP™, TriCore™.

**Other Trademarks**

Advance Design System™ (ADS) of Agilent Technologies, AMBA™, ARM™, MULTI-ICE™, KEIL™, PRIMECELL™, REALVIEW™, THUMB™, µVision™ of ARM Limited, UK. AUTOSAR™ is licensed by AUTOSAR development partnership. Bluetooth™ of Bluetooth SIG Inc. CAT-iq™ of DECT Forum. COLOSSUS™, FirstGPS™ of Trimble Navigation Ltd. EMV™ of EMVCo, LLC (Visa Holdings Inc.). EPCOS™ of Epcos AG. FLEXGO™ of Microsoft Corporation. FlexRay™ is licensed by FlexRay Consortium. HYPERTERMINAL™ of Hilgraeve Incorporated. IEC™ of Commission Electrotechnique Internationale. IrDA™ of Infrared Data Association Corporation. ISO™ of INTERNATIONAL ORGANIZATION FOR STANDARDIZATION. MATLAB™ of MathWorks, Inc. MAXIM™ of Maxim Integrated Products, Inc. MICROTEC™, NUCLEUS™ of Mentor Graphics Corporation. MIPI™ of MIPI Alliance, Inc. MIPS™ of MIPS Technologies, Inc., USA. muRata™ of MURATA MANUFACTURING CO., MICROWAVE OFFICE™ (MWO) of Applied Wave Research Inc., OmniVision™ of OmniVision Technologies, Inc. Openwave™ Openwave Systems Inc. RED HAT™ Red Hat, Inc. RFMD™ RF Micro Devices, Inc. SIRIUS™ of Sirius Satellite Radio Inc. SOLARIS™ of Sun Microsystems, Inc. SPANSION™ of Spansion LLC Ltd. Symbian™ of Symbian Software Limited. TAIYO YUDEN™ of Taiyo Yuden Co. TEAKLITE™ of CEVA, Inc. TEKTRONIX™ of Tektronix Inc. TOKO™ of TOKO KABUSHIKI KAISHA TA. UNIX™ of X/Open Company Limited. VERILOG™, PALLADIUM™ of Cadence Design Systems, Inc. VLYNQ™ of Texas Instruments Incorporated. VXWORKS™, WIND RIVER™ of WIND RIVER SYSTEMS, INC. ZETEX™ of Diodes Zetex Limited.

Last Trademarks Update 2011-11-11

## Table of Content

<b>1</b>	<b>Introduction .....</b>	<b>6</b>
<b>2</b>	<b>System description and measurement setup .....</b>	<b>8</b>
2.1	System description .....	8
2.1.1	Standby state .....	9
2.1.2	VCO settling time .....	10
2.1.3	Sampling .....	10
2.1.4	Data processing .....	10
2.2	Measurement setup .....	11
<b>3</b>	<b>Measurement results .....</b>	<b>13</b>
3.1	Effect of temperature variation on the VCO settling time to the ISM band $t_{VCO}$ .....	13
3.2	Sampling time $t_{sample}$ .....	21
3.3	Summary of measurement results .....	22
<b>4</b>	<b>Conclusion .....</b>	<b>22</b>
<b>5</b>	<b>References .....</b>	<b>24</b>
<b>6</b>	<b>Author .....</b>	<b>24</b>

## List of Figures

Figure 1	BGT24MTR11's power consumption as a function of measurement update time. ....	6
Figure 2	Pulsed mode Doppler Radar setup .....	8
Figure 3	Duty-cycle operation of the Radar system .....	9
Figure 4	High-side load switch .....	11
Figure 5	Block diagram of the measurement setup .....	12
Figure 6	Microcontroller firmware structure and timings .....	12
Figure 7	TX spectrum using the <i>max hold</i> function. The VCO is controlled by the DACs. The temperature was varied over time.....	13
Figure 8	Expected temperature variation in pulsed-mode. ....	14
Figure 9	TX spectrum with $T_{ON} = 15$ s and $T_{OFF} = 15$ s. ....	15
Figure 10	TX spectrum with $T_{ON} = 32$ ms and $T_{OFF} = 0.5$ s. ....	15
Figure 11	TX spectrum with $T_{ON} = 32$ ms and $T_{OFF} = 1$ s. ....	16
Figure 12	TX spectrum with $T_{ON} = 32$ ms and $T_{OFF} = 2$ s. ....	16
Figure 13	TX spectrum with $T_{ON} = 32$ ms and $T_{OFF} = 4$ s. ....	17
Figure 14	BGT24 VCO center frequency and frequency drift as a function of temperature .....	18
Figure 15	Spectrogram of oscilloscope data with $t_{ON} = 130$ ms and $t_{OFF} = 300$ ms .....	19
Figure 16	Figure 15 enlarged around the relevant frequency value. ....	19
Figure 17	Spectrogram of oscilloscope data with $t_{ON} = 4.5$ s and $t_{OFF} = 1$ s. ....	20
Figure 18	Temperature variation as a function of time with $t_{ON} = 4.5$ s and $t_{OFF} = 1$ s. ....	20
Figure 19	Simulation of the frequency estimation over the velocity range of interest with $SNA = 5$ dB, $f_{sample} = 5$ KSps and $t_{sample} = 9$ ms. ....	22

## List of Tables

Table 1	Design goals.....	6
Table 2	Resulting Doppler shift and minimum measurement time for different speeds .....	7
Table 3	XMC4500 power modes.....	10
Table 4	Measured occupied bandwidths for different $t_{OFF}$ values. ....	17



## 1 Introduction

In this study, the feasibility of a battery powered low-power 24 GHz Doppler radar based on the BGT24MTR11 chip was evaluated. The operating scenario is the detection of human body movement through velocity. Possible applications are security and surveillance systems and automatic lighting applications, which basically needs to detect the presence of a person within a defined range. The underlying design goals are as mentioned in Table 1.

**Table 1 Design goals**

Parameter	Design goal
Speed range	2.5 km/h – 20 km/h
Doppler shift	111 Hz – 888 Hz
Measurement rate	2 Hz (2 updates / second)
Temperature range	-40 °C - 105 °C
Output power	11 dBm (max. output power of BGT24MTR11)
Speed uncertainty	1 km/h

In order to reduce the power consumption, the radar chip has to be operated in a duty-cycling mode; that means that measurements are conducted within short intervals separated by sleep times in which the radar chip is unpowered.

**This document shows that it is possible to reach these design goals in a duty-cycling mode, so that the radar chip is activated for about 10 ms and shut down for the remaining 490 ms, reducing the power consumption in this mode to only 2% of what would otherwise be required in continuous operation.**

**This is equivalent to a power reduction from 528 mW needed in the continuous mode, with maximum output power and current consumption of the BGT24MTR11, down to merely 12 mW when the radar is operated in the duty-cycling mode, while providing the maximum output power of the IC.**

Due to the fact that we use here a simple radar system without frequency modulation and a comparably low measurement rate this document serves as a kind of an estimation of the lower limit of power consumption that is possible with the BGT24MTR11.

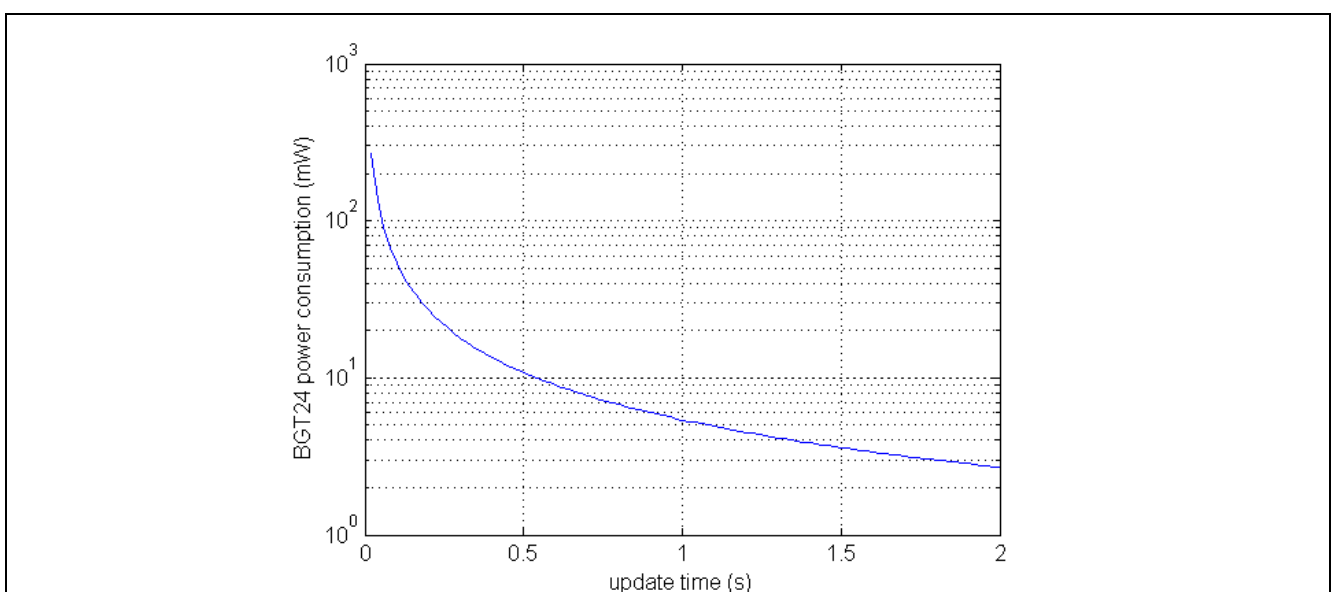


**Figure 1 BGT24MTR11's power consumption as a function of measurement update time.**

The duty-cycle mode described here can also be applied to the other siblings of Infineon Technologies 24 GHz-radar family.

The optimization of digital software and hardware as well as other components will not be discussed in this document. Solely the power consumption of the radar chip will be taken into account.

Figure 1 shows the power consumption as a function of the measurement update time. For example, an update time of 0.5 s means there is a new measurement every 0.5 s. The graph implies an assumed activation time of 10 ms. It should be mentioned that the power consumption values affect only the radar chip and not the complete radar system. Depending on the application, the power consumption may be further reduced using a lower TX output power, this leads however to a reduced coverage range of the radar.

Table 2 gives an overview on the Doppler frequencies generated by targets with different speed and the minimum measurement time required to be able to measure those speeds correctly. It shows that a finer speed resolution needs a longer measurement time.

**Table 2 Resulting Doppler shift and minimum measurement time for different speeds**

Speed	km/h	1	1.5	2	2.5	3	4	5	6	8	10
Doppler shift	Hz	44.4	66.7	88.9	111.1	133.3	177.8	222.2	266.7	355.6	444.4
Min. measurement time	ms	22.5	15.0	11.3	9.0	7.5	5.6	4.5	3.8	2.8	2.3

## 2 System description and measurement setup

### 2.1 System description

The proposed radar system setup is described in Figure 2. The radar system consists of the BGT24MTR11 radar IC, a baseband amplifier, the Infineon XMC4500 Cortex-M4 microcontroller and a load switch connected to the 3.3 V supply input of the BGT24. Only the used ports of the BGT24MTR11 are represented in Figure 2.

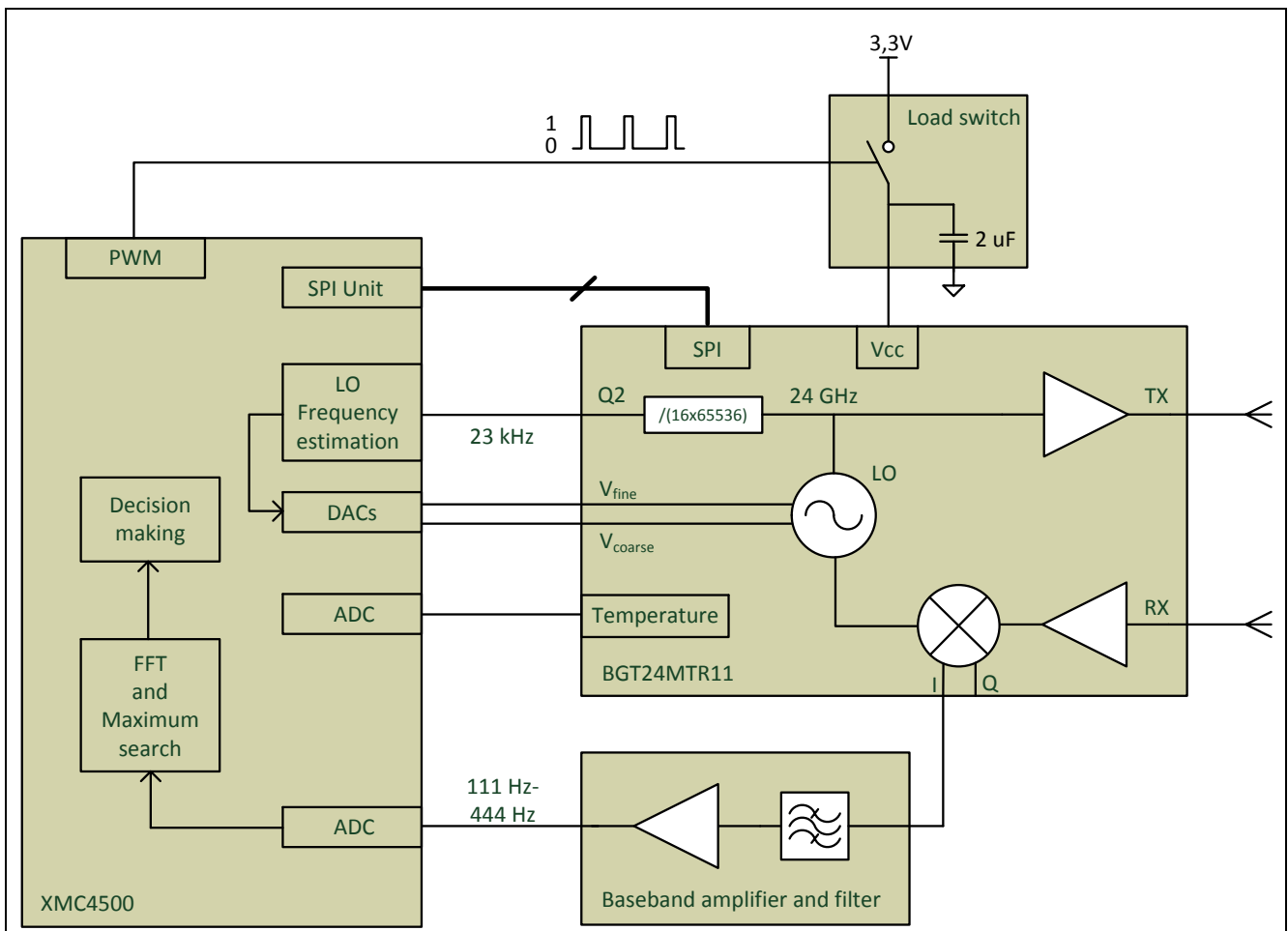


**Figure 2 Pulsed mode Doppler Radar setup**

The VCO's (voltage controlled oscillator) tuning voltages are controlled directly by the DACs (Digital-to-analog converter) of the XMC4500. The 23 kHz digital prescaler output is used by the microcontroller to estimate the VCO frequency. The frequency estimation may be implemented through counting the rising and falling edges over a time interval. The result is then compared to the reference microcontroller clock generated using a precise crystal oscillator. The SPI interface is used to program the BGT24's registers (output power setting, enable PA, multiplexer settings, etc.). The load switch is controlled by the microcontroller and is used to connect or disconnect the BGT24 to and from the supply voltage. The temperature of the chip can be monitored by the microcontroller using the integrated temperature sensor. The temperature sensor may be powered by an external supply, thus allowing the temperature monitoring even when the radar chip is switched off. The baseband module is used to amplify the baseband Doppler signal so that it matches the ADC input range and to filter the frequency equivalents of unwanted velocities.

Since the direction of the movement is not essential for this application, only the In-phase (I) component of the signal was amplified, digitized and processed to reduce the cost and power consumption of the system.



The microcontroller is responsible for the complete system control, data acquisition and data processing. The operation of the radar is described in the following sections.

The pulsed radar operation cycle is highlighted in Figure 3. It consists of four different states with different power consumption:

- Standby
- VCO settling
- Sampling
- Data processing

States with high power consumption are drawn in red, with medium power consumption in yellow and with lowest power consumption in green. During standby the power consumption of the system is low. After a certain time in standby mode the microcontroller is woken up by a timer interrupt and turns on the BGT24-IC. During VCO settling the PA output of BGT24MTR11 is kept disabled until the VCO's frequency is inside the ISM Band. Then transmission of the signal is enabled and the received and down-converted signal is being sampled. VCO settling and sampling are the two states with the highest power consumption. Once sampling is complete the BGT24 is tuned off and the microcontroller processes the sampled data. After decision – a target is present or not – the system goes back into standby mode.

The four states will be discussed in more detail in the next section.

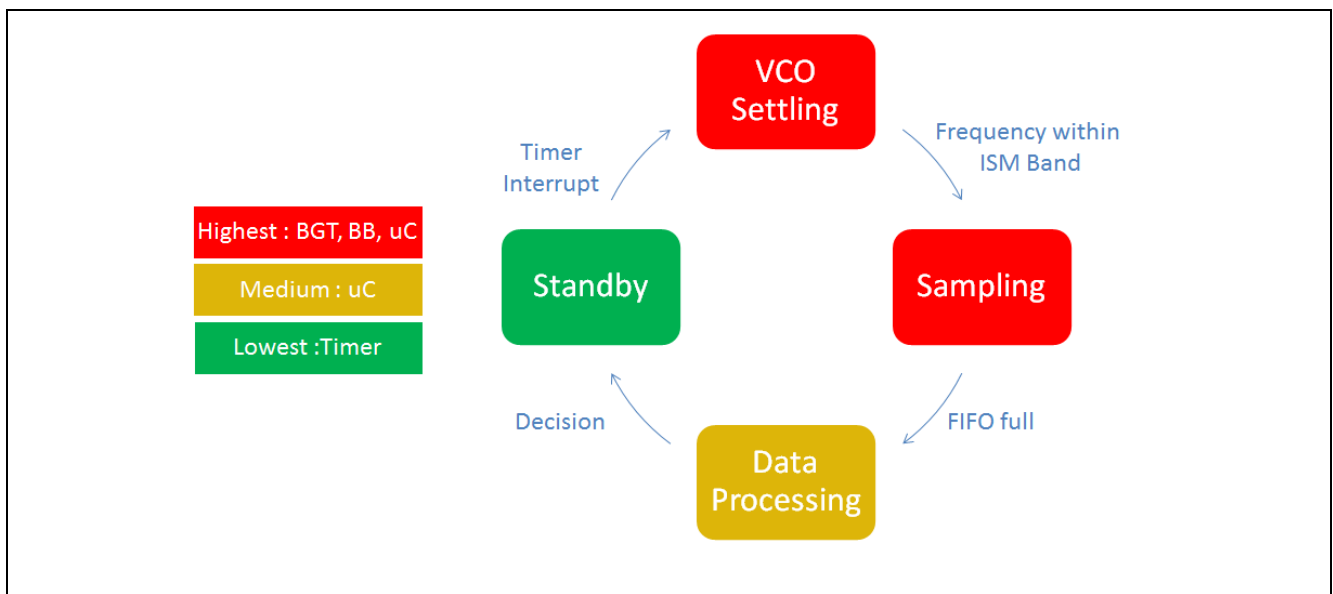


**Figure 3** Duty-cycle operation of the Radar system

### 2.1.1 Standby state

The standby state is the time slot of duration  $t_{OFF}$  at which the power consumption is reduced to a very low value. During the relatively long stand-by time, BGT24MTR11 and the base band amplifier are disconnected from the 3.3 V supply source. The microcontroller is set to a sleep mode or hibernated and its function is reduced to a timer that wakes up the system within regular time intervals through an interrupt. When using the XMC4500 multiple power-management modes are available [2]:

- **Sleep mode:** Processor clock is stopped.
- **Deep sleep mode:** System clock is stopped and PLL, as well as flash, are switched off.
- **Hibernate:** The power supply to the core is switched off. The RTC (Real Time Clock) may be used to wake up the microcontroller to the active state (RTC periodic event).

Table 3 summarizes the typical supply currents and wake-up times for the different states.

**Table 3 XMC4500 power modes**

MCU power mode	Supply current	Wake-up time
Active	110 mA / 180 mA (typ./worst case at f = 120 MHz)	-
Sleep	46 mA (f = 100 kHz)	6 cycles
Deep sleep	6 mA (f = 100 kHz)	270 μs (flash memory wake-up time)
Hibernate (RTC on)	10 μA (V <sub>BATT</sub> = 3.3 V)	3.5 ms (max.)

### 2.1.2 VCO settling time

The microcontroller uses one of its internal timers at a pre-defined rate to activate the measurements by connecting the radar IC and the baseband module to the 3.3 V power supply.

In BGT24MTR11's default power-on state, the PA (power amplifier) outputs of the TX signal are disabled. This prevents transmitting power outside the ISM band right after power-up when the TX frequency might not be controlled yet. Only after the VCO has settled to the target frequency the TX outputs should be enabled.

In conjunction with a Doppler radar, the VCO frequency's exact value is not critical to the measurement accuracy and leads to measurement errors below 0.12 km/h. This assumption is valid, when a VCO frequency of 24.125 GHz is assumed and the unknown actual frequency is between 24 GHz and 24.25 GHz.

It must be ensured, however, that the output frequency remains within the limits of the ISM band (24 GHz – 24.25 GHz). Therefore the PA should remain disabled for a time interval  $t_{VCO}$  until the microcontroller verifies, using the 23 kHz prescaler output, that the VCO frequency is within the allowed ISM frequency band. The ISM band is equivalent to a prescaler frequency range of [22.888 kHz – 23.127 kHz]. Using the much higher microcontroller clock (in the MHz range), the prescaler frequency may be accurately estimated with about 5 frequency periods (about 217 μs).

### 2.1.3 Sampling

Once the VCO frequency is within the ISM band, the power amplifier may be enabled and the baseband signal is sampled by an analog-to-digital converter (ADC). During this time, the microcontroller core may be deactivated and only the peripherals (ADC, DAC, SPI, etc.) remain active in order to further reduce the power consumption. The ADC reactivates the core through an interrupt.

### 2.1.4 Data processing

After the sampling, the BGT24 and the baseband module are turned off again and the data is processed within the microcontroller to extract the velocity information. The main blocks of the processing are the FFT (Fast Fourier Transform) and the maximum search of its magnitude. The maximum value is then compared to a threshold, and when exceeded, the presence of a moving human in the radar vicinity is assumed valid.

## 2.2 Measurement setup

The used measurement setup is very similar to the actual radar setup as in Figure 2. The setup was realized using:

- **BGT24MTR11 evaluation board:** Three similar evaluation boards were used to verify the reproducibility of the measurements.
- **XMC4500 microcontroller Hexagon Board:** Together with the pin extension card and the J-Link Lite Debugger: Used for controlling BGT24MTR11, as well as for signal acquisition and data processing. The Infineon Dave 3 programming interface was used to program and debug the code. The measurement results were communicated to a computer through the USB interface.
- **Baseband amplifier and filter:** Serves as an interface between the BGT24's IF outputs and the ADC input. Operational amplifiers with a single supply voltage equal to that of the BGT24 (3.3 V) are advantageous. Furthermore it is beneficial to choose rail-to-rail amplifiers to cover the whole input range of the ADC.
- **A load switch** to connect and disconnect BGT24MTR11 to the power supply. The load switch should have a control voltage and an operating voltage of 3.3 V. A typical switch consists of both an N-channel and a P-channel (power) MOSFET according to Figure 4. In the implemented prototype board, an integrated solution incorporating both switches in a small package was used. When connected to BGT24MTR11, the measured rise time of the switch output is about 55  $\mu$ s.
- 

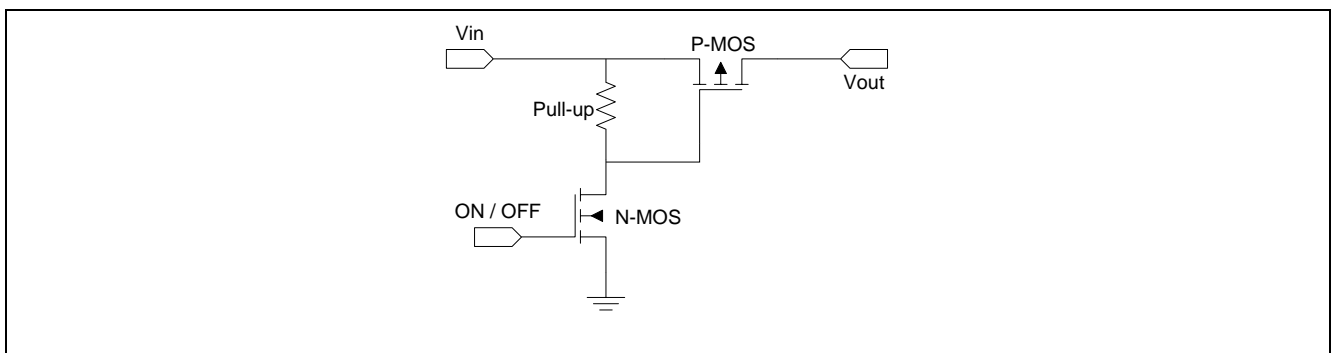


**Figure 4 High-side load switch**

A block diagram of the measurement setup is shown in Figure 5. The In-phase component of the baseband signal (IF\_I / IF\_IN) is connected to an ADC channel of the microcontroller. The quadrature component was left unconnected to reduce the power that otherwise would have been required by a second baseband amplifier, by a second ADC channel as well as additional processing time and resources.

An oscilloscope is used to measure the 23 kHz output (actual VCO frequency/16/65536) of the BGT24 as well as the 1.5 GHz output. The oscilloscope measures also the temperature sensor output to monitor the temperature variation during ON-OFF switching of the BGT24. The temperature sensor has a sensitivity of 3-4 mV/K and is, as already mentioned, independently biased to allow temperature measurements even when the BGT24 is in the OFF state.

One of the differential TX ports was terminated by a 50  $\Omega$  load, the other was connected to the input of a spectrum analyzer to measure the amplitude and the frequency of the transmitted signal. The used coaxial SMA cable has an insertion loss of 11 dB at 24.125 GHz. The spectrum analyzer not only serves to track the instantaneous frequency but also to capture the frequency variation over some time interval by using the *max hold* function.

The microcontroller acts as a master. The Digital-to-Analog converters (DACs) are connected through low-pass RC filters ( $R = 100 \Omega$  and  $C = 1 \mu$ F) to the VCO coarse and fine inputs. The sampling frequency of the ADCs was set to 5000 Sps (Samples per second).

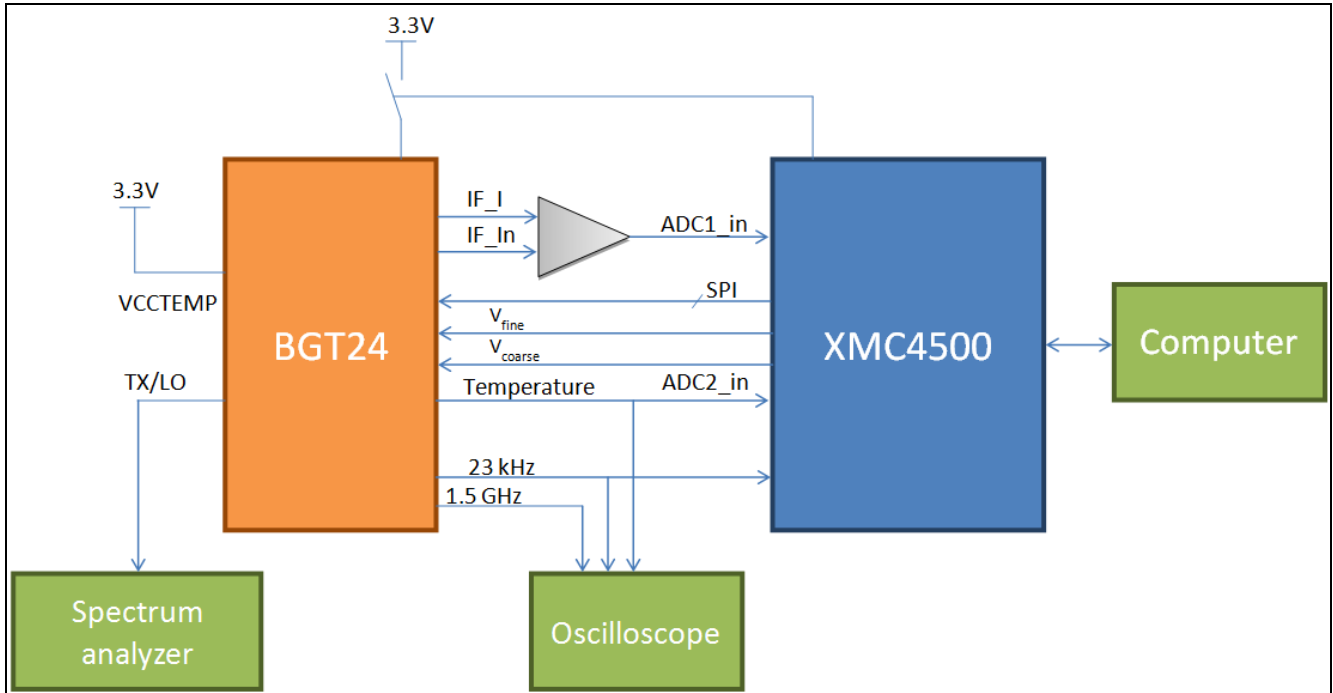


**Figure 5** Block diagram of the measurement setup

The firmware structure including the timing of the different steps is described in Figure 6. Right after the start of the complete system the DACs are activated and they provide a tuning voltage bigger than 0.5 V to make sure that the voltage at the tuning pins is high enough for the VCO to fire. For more details please refer to the VCO section in [1]. Then the analog radar front-end is switched on and the system waits for the VCO frequency to settle in the ISM-band. This is done by a software loop. The XMC4500 reads out the frequency provided by the Q2-prescaler (~23 kHz), which corresponds to the VCO frequency divided by  $2^{20}$ , and changes the tuning voltages until the VCO's frequency is at the desired value. Once this is completed, the PA of BGT24 is enabled via the SPI-bus and the actual measurement takes place. After the received signal is sampled and stored the analog frontend is switched off again and the XMC processes the received data and goes into sleep mode when finished. After the desired standby time the next measurement sequence is being started.

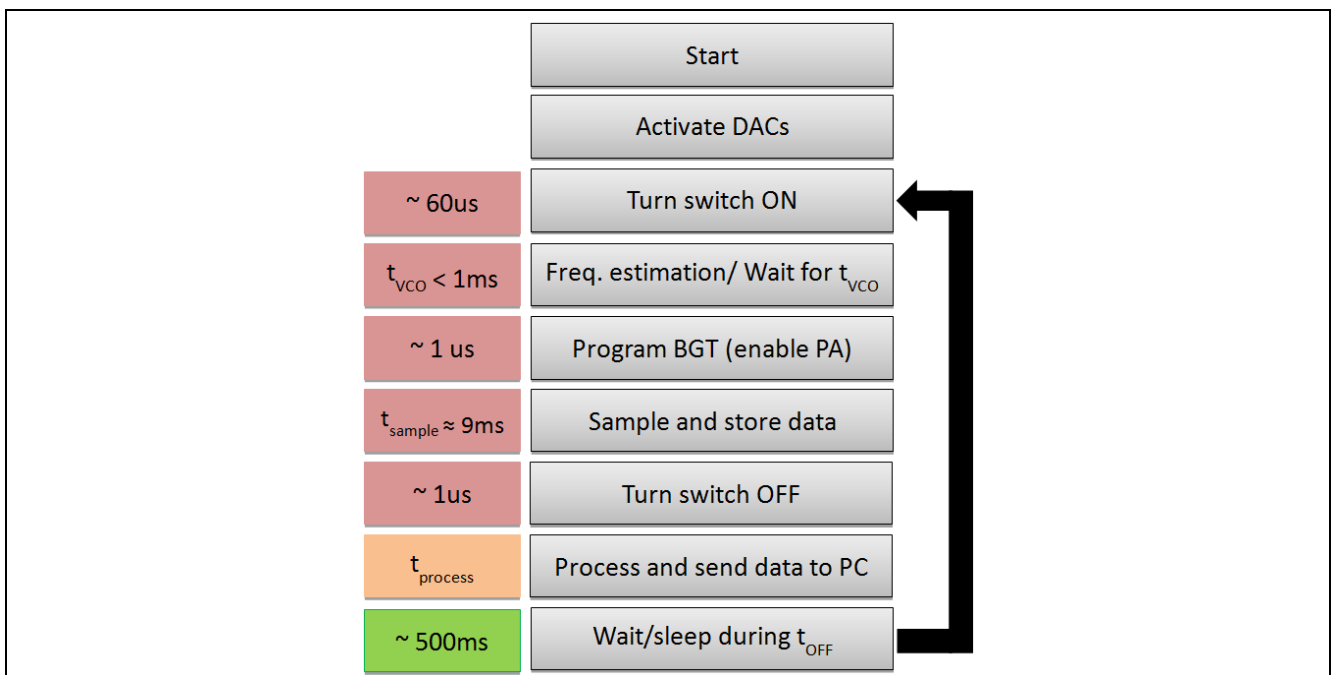


**Figure 6** Microcontroller firmware structure and timings

### 3 Measurement results

The total BGT ON time is expressed by

$$t_{ON} = t_{RISE} + t_{VCO} + t_{SPI} + t_{Sample}$$

With a measurement rate of 2 Hz, the duration of a cycle is about  $t_{cycle} = 500$  ms.  $t_{SPI}$  and  $t_{RISE}$  are considerably smaller than  $t_{cycle}$  and will not be considered any further.

#### 3.1 Effect of temperature variation on the VCO settling time to the ISM band $t_{VCO}$

$t_{VCO}$  is the time needed by the VCO frequency to settle within the ISM frequency band (24 GHz – 24.25 GHz). The VCO covers frequencies up to 26 GHz and may easily drift outside the band mainly due to temperature variations. The temperature variation may be caused by the environment, for example by neighboring electronic components or by the radar chip itself due to power dissipation. It should be noted that only relatively fast temperature variations are of interest in our discussion since slow variations are compensated in relatively long time intervals through the 23 kHz feedback path.

The measurement setup of Figure 5 was used to verify the behavior of the VCO output frequency under strongly varying temperatures while maintaining a constant control voltage. The picture shows the captured TX spectrum using the *max hold* function of the spectrum analyzer to capture all the VCO frequencies over a time interval. At room temperature the frequency was set by the DACs to 24.125 GHz, the middle of the ISM band. The chip temperature was then varied using a freeze spray (down to about -30 °C) for low temperatures and hot air (up to 100 °C) for higher temperatures. The VCO frequency variation goes beyond the ISM band bounds (Marker 1 and 2 for the lower and upper limits). This implies that, in general, the VCO of the BGT24 may not be operated over a large temperature range using a free running mode without any feedback path to control the frequency.

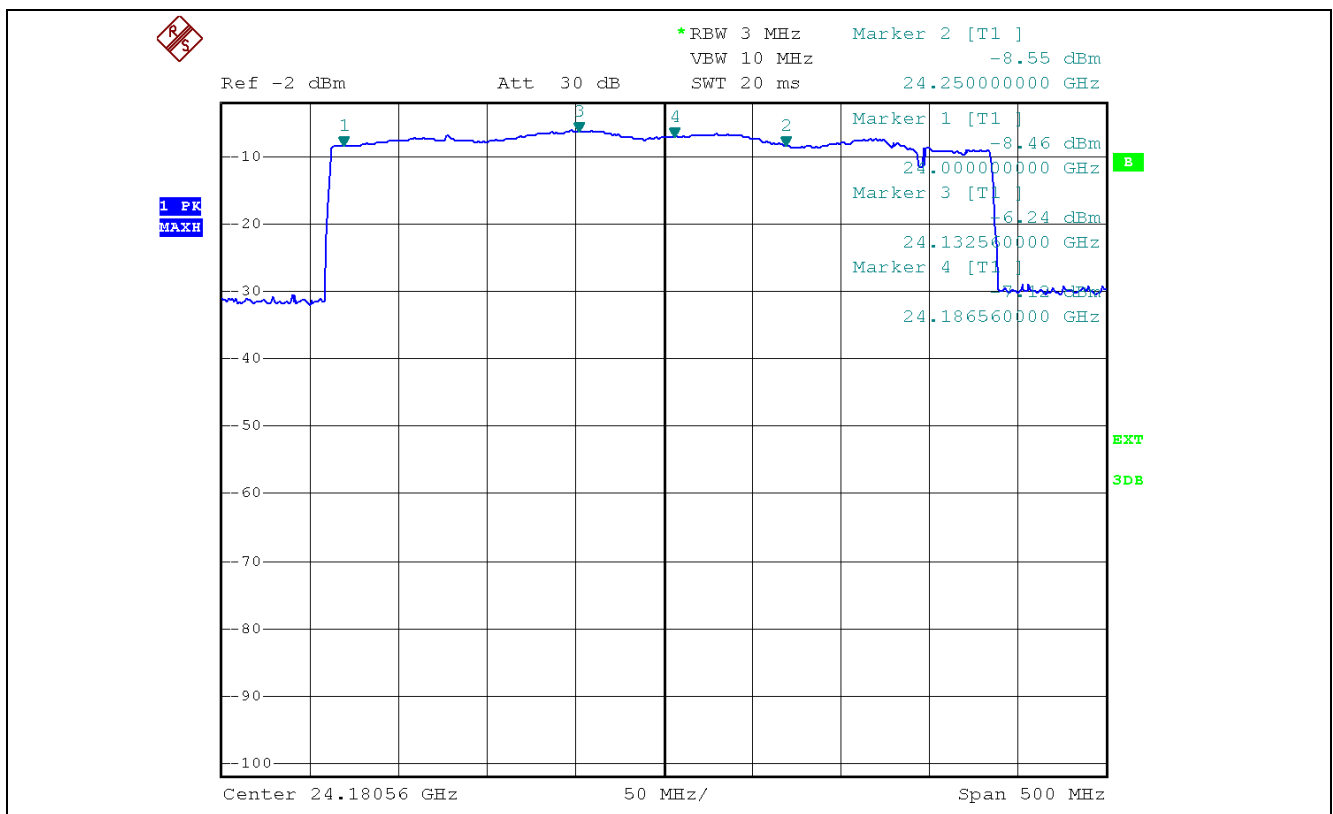


**Figure 7 TX spectrum using the *max hold* function. The VCO is controlled by the DACs. The temperature was varied over time.**

It was observed that, using continuously running radar without any external temperature variation, the frequency drift at the steady state did not exceed about 15 MHz in the worst case. In this case the calibration may be applied within relatively large time intervals since the VCO operates in a stable operating temperature.

The duty-cycle mode results, however, in a rapidly changing temperature due to the alternating power dissipation of the radar chip leading to cyclic variations of the VCO temperature. The temperature depends on the ON and OFF state durations as well as multiple other parameters such as heat transfer properties of the PCB, TX power, etc.. Figure 8 represents the expected temperature variation of the BGT in the pulsed mode.  $T^{\circ}_{ON,ss}$  and  $T^{\circ}_{OFF,ss}$  are the steady state temperatures of the ON and OFF states respectively reached after a relatively long time after which the chip temperature remains constant. During the pulse operation the temperature varies between both steady state values depending on the ON and OFF interval lengths. The highest temperature variations should be reached when both state durations are relatively long, as the VCO frequency varies monotonically with temperature [1].

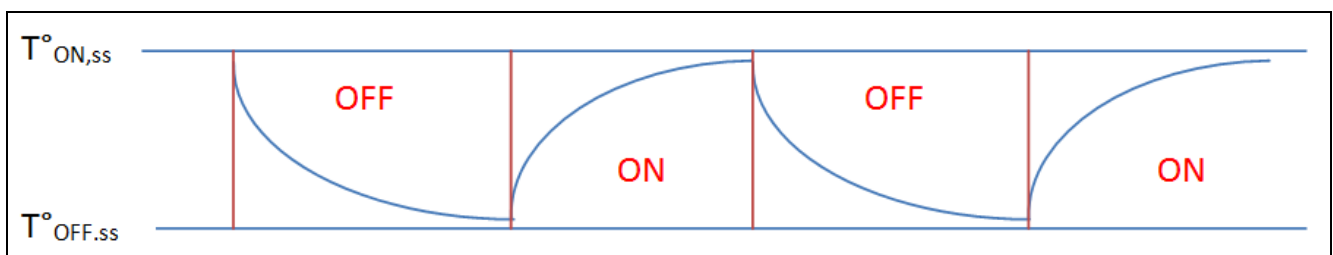


**Figure 8** Expected temperature variation in pulsed-mode.

This frequency variation was measured first using the spectrum analyzer and the *max hold* function. The observation time was made long (few minutes) to make sure all occurring frequencies are captured. The measured spectrum was then compared to the ISM bandwidth. As the measured bandwidth was smaller than the ISM band,  $t_{VCO}$  may be set to zero, i.e. the BGT24 power amplifier may be turned ON almost immediately after powering the VCO, given that the ambient temperature didn't change since the last measurement cycle.

The maximum occupied bandwidth variation should be observed when the largest values of  $t_{OFF}$  and  $t_{ON}$  are used. Figure 9 shows the bandwidth measurement for  $t_{OFF} = t_{ON} = 15$  s. The cycle length is sufficiently large to reach a steady operating temperature for both the ON and the OFF state. The measured bandwidth is about 80 MHz and therefore considerably less than the available bandwidth of the ISM band.

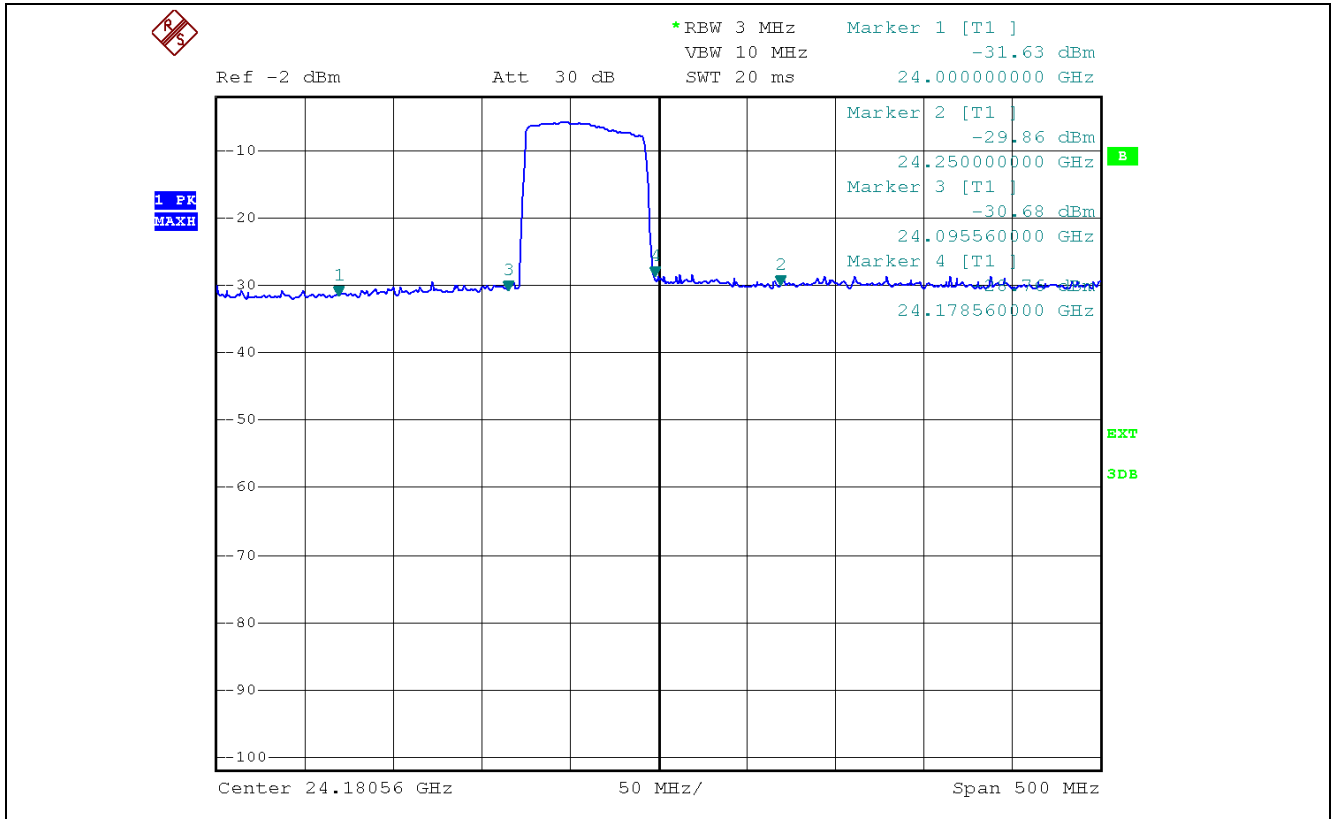


**Figure 9** TX spectrum with  $T_{ON} = 15$  s and  $T_{OFF} = 15$  s.

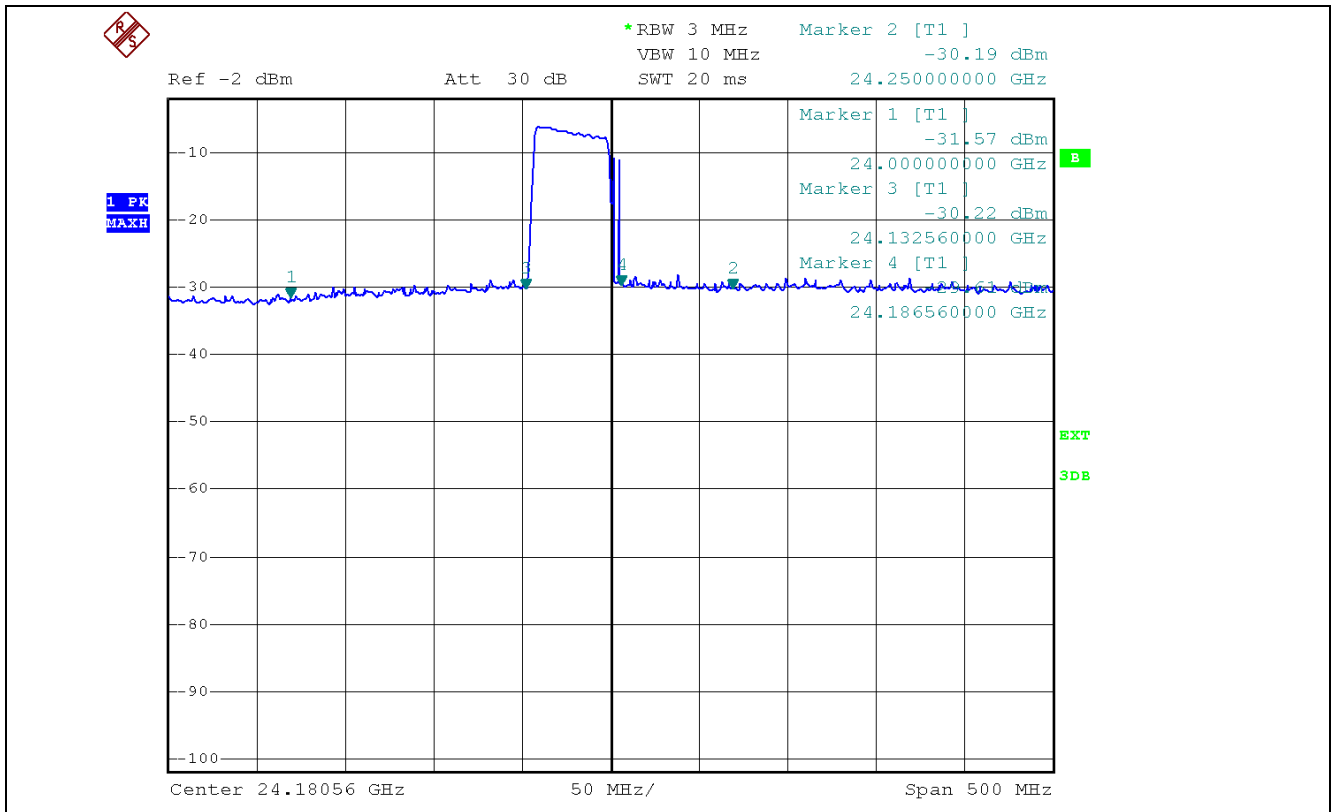


**Figure 10** TX spectrum with  $T_{ON} = 32$  ms and  $T_{OFF} = 0.5$  s.

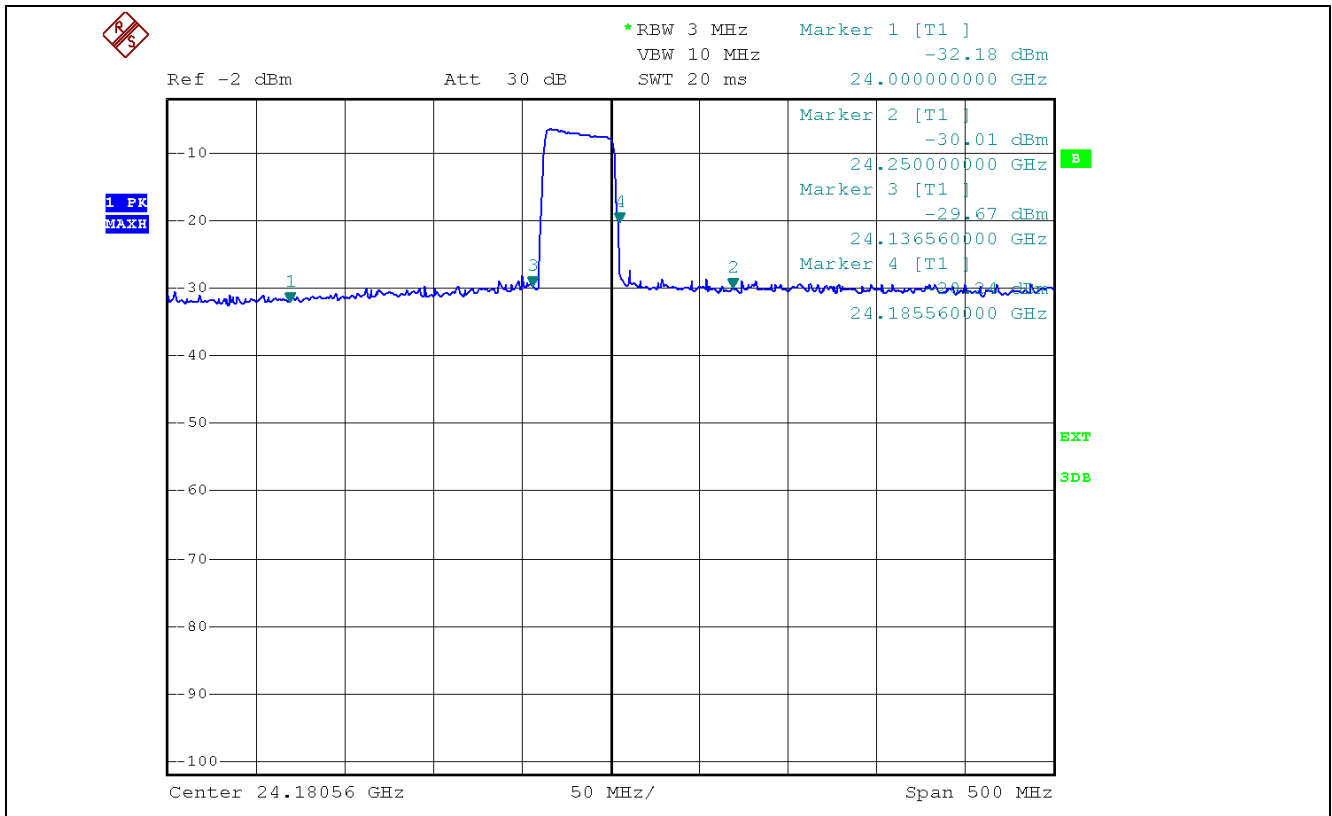


**Figure 11 TX spectrum with  $T_{ON} = 32$  ms and  $T_{OFF} = 1$  s.**

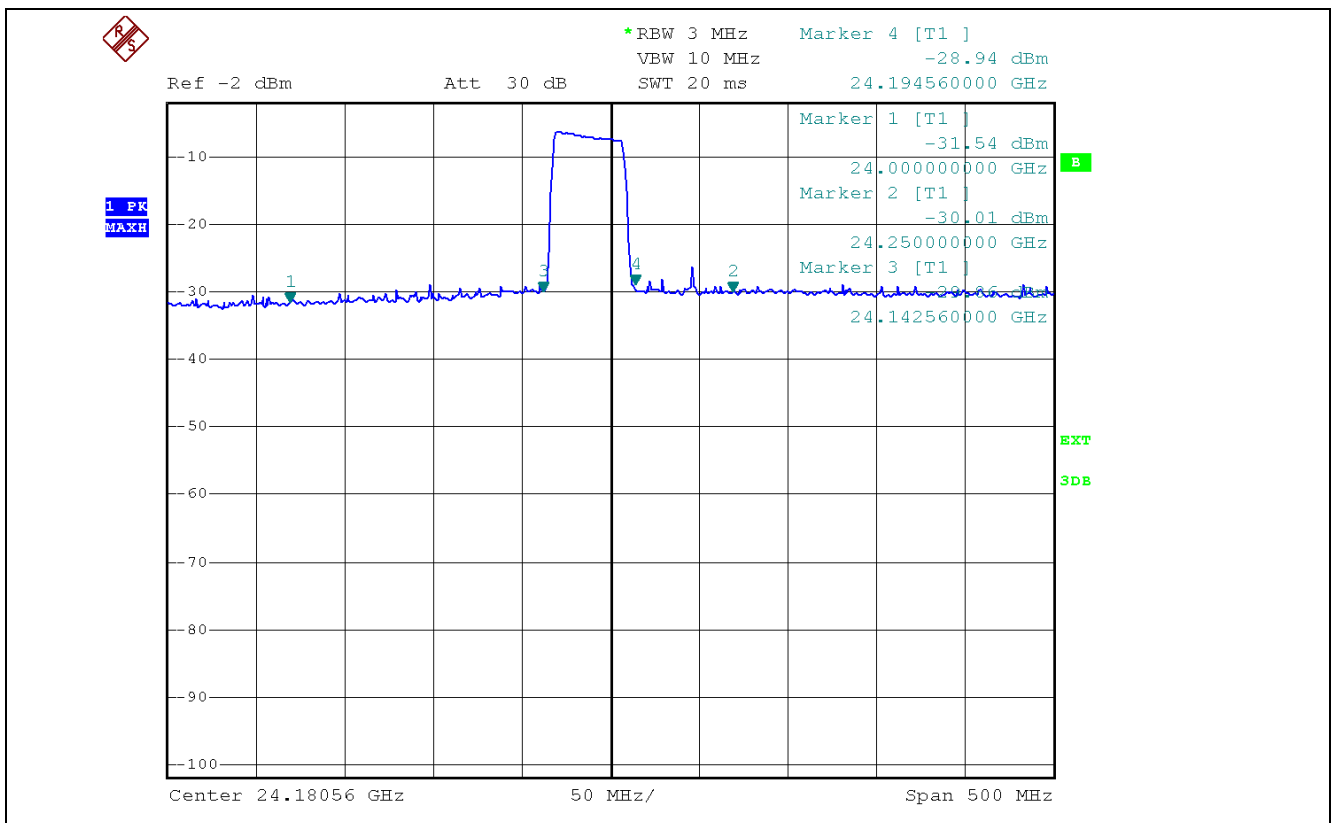


**Figure 12 TX spectrum with  $T_{ON} = 32$  ms and  $T_{OFF} = 2$  s.**



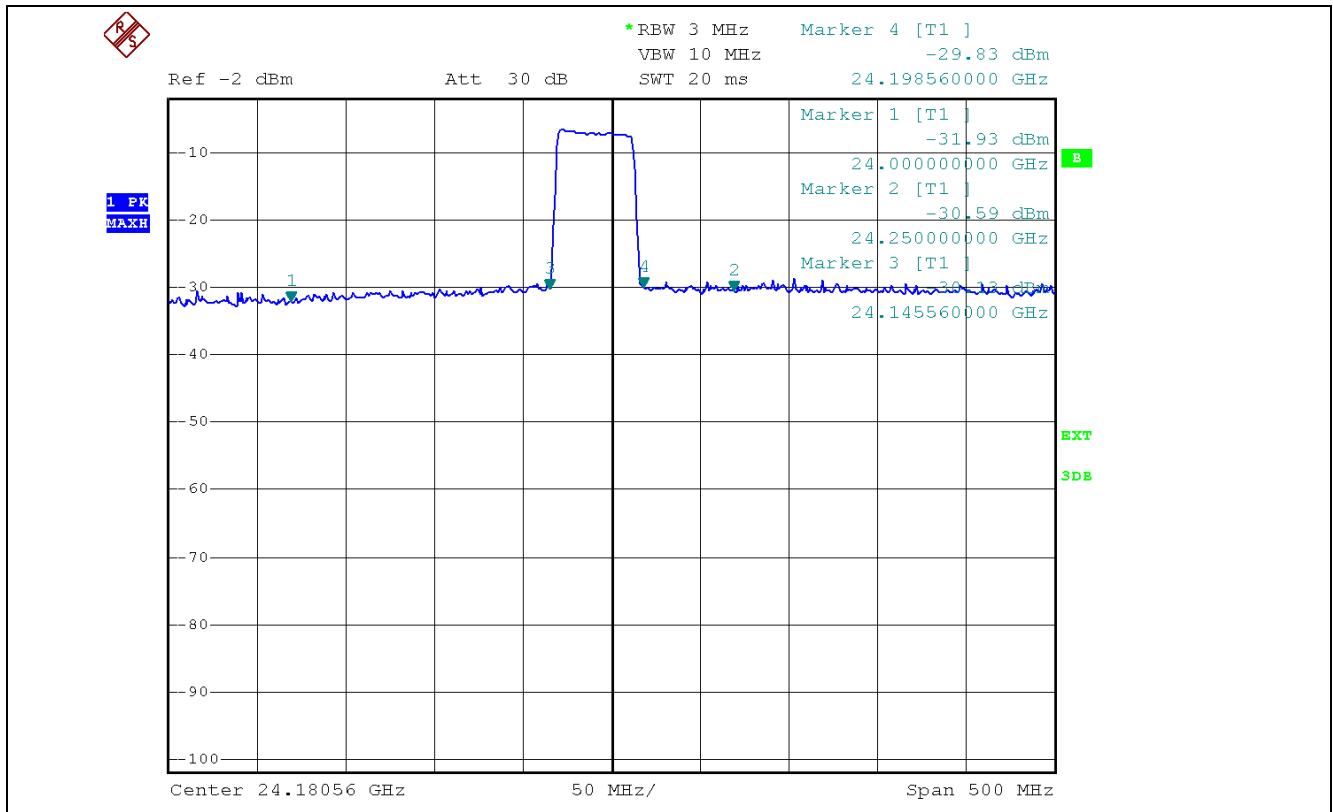


**Figure 13** TX spectrum with  $T_{ON} = 32$  ms and  $T_{OFF} = 4$  s.

Measurements using shorter cycles were performed and measured bandwidths were, as expected, smaller than in Figure 9. Measurements results are shown in Figure 9 - 13 and in Table 4.  $t_{ON}$  was set fixed to 32 ms.  $t_{OFF}$  has been varied between 0.5 s to 4 s. A lower  $t_{ON}$  value would lead to an even smaller occupied bandwidth since the radar chip would not reach higher temperatures.

**Table 4** Measured occupied bandwidths for different  $t_{OFF}$  values.

$t_{ON}$	32 ms	32 ms	32 ms	32 ms	15 s
$t_{OFF}$	0.5 s	1 s	2 s	4 s	15 s
BW	49 MHz	52 MHz	53 MHz	54 MHz	80 MHz
Figure	Figure 10	Figure 11	Figure 12	Figure 13	Figure 9

These measurements were verified over the temperature range [-30°C - +85°C] using a temperature forcing system to maintain a steady ambient temperature. During the measurement the tuning voltage of the VCO was kept to a fixed value.

The results are plotted in Figure 14 and show that, as expected, the center frequencies are partially located outside the ISM band due to the temperature variation. The frequency drift using a pulsed mode with  $t_{ON} = t_{OFF} = 15$  s shows to the variations depicted as vertical bars in Figure 14. The frequency drift, measured at a steady ambient temperature, does not exceed 50 MHz. The frequency drift remains significantly lower than the available ISM bandwidth of 250 MHz.

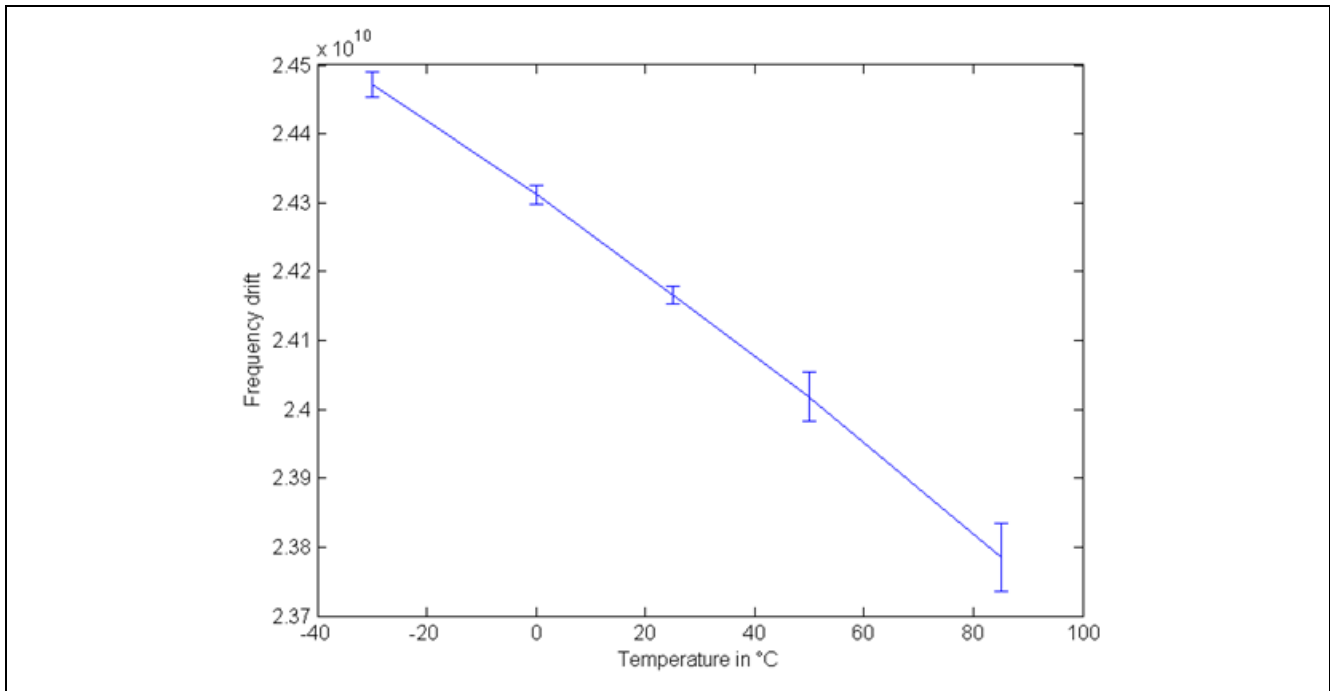


**Figure 14 BGT24 VCO center frequency and frequency drift as a function of temperature**

In order to verify the spectrum analyzer measurements, the 23 kHz prescaler output data was captured using a digital oscilloscope. The frequency relates to the VCO frequency through

$$f(\text{prescaler}) = \frac{f(\text{VCO})}{65536 \times 16} = \frac{f(\text{VCO})}{1048576} \quad (1)$$

In order to measure the frequency variation over time using the time domain data, short time Fourier transforms with overlapping intervals were applied. The extracted data shows not only the occupied frequencies but also their variation with time. The parameters of the short time Fourier Transform should be carefully chosen so that the measured frequency is accurate. The MATLAB spectrogram function may be used to plot the frequency-time dependency. Figure 15 shows the frequency variation over time for a pulsed mode with  $t_{\text{ON}} = 130$  ms and  $t_{\text{OFF}} = 300$  ms. The frequency, depicted with the white line, is the maximum of the Fourier transform and shows a variation of about 20 Hz, where the red area is equivalent to the ON state. Equivalently, the TX bandwidth varies according to (1) by about 21 MHz and remains therewith inside the ISM band. The figure shows also a frequency variation at the end of the ON interval caused by the ON-OFF switching. This is apparently due to the VCO control voltage variation caused through the chip internal pull-up resistors. This effect may be avoided by disabling the PA before switching off the supply voltage.

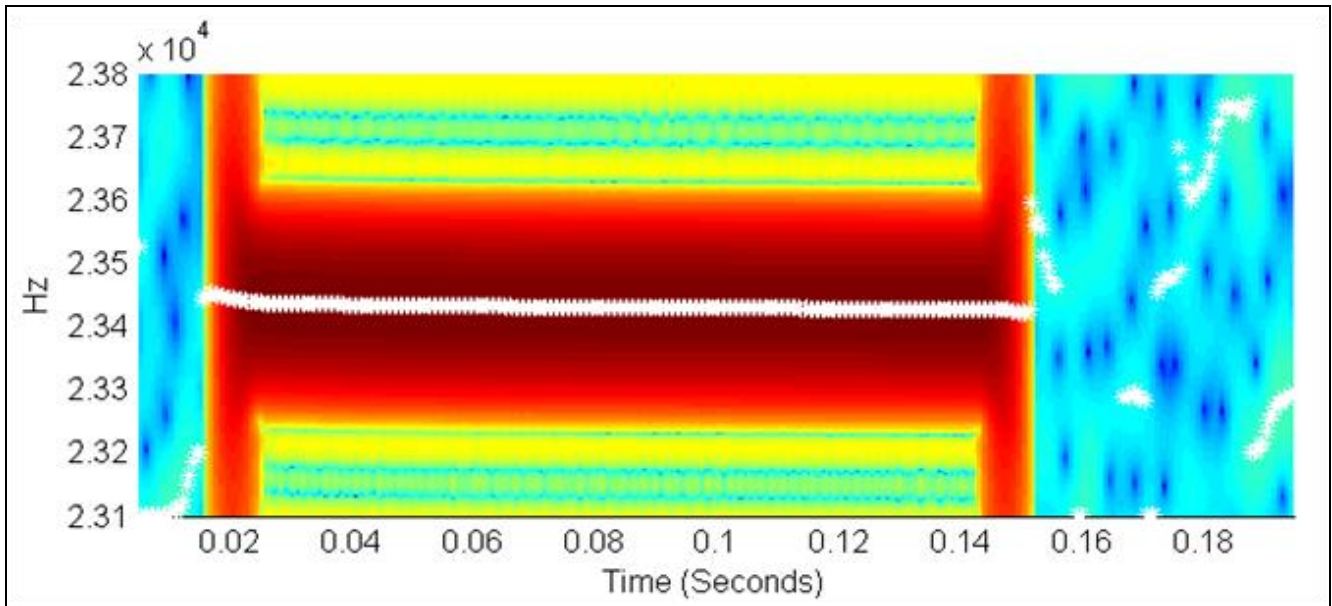


**Figure 15** Spectrogram of oscilloscope data with  $t_{ON} = 130$  ms and  $t_{OFF} = 300$  ms

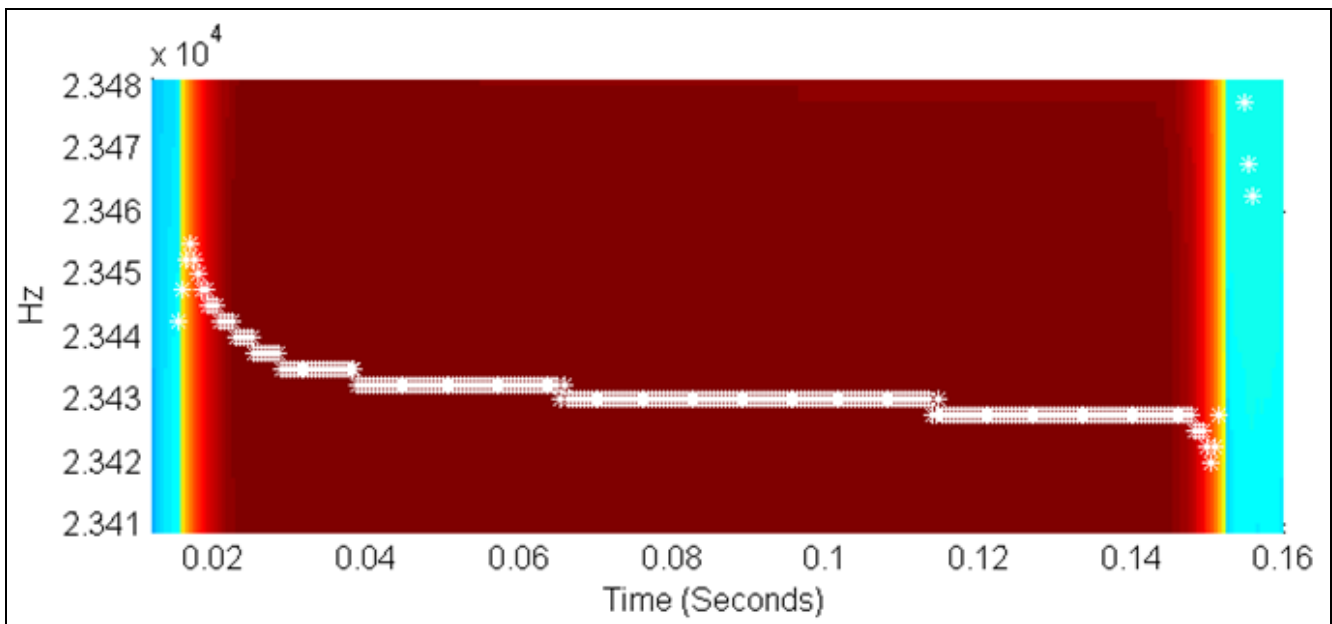


**Figure 16** Figure 15 enlarged around the relevant frequency value.

In Figure 17, the slow frequency variation over the ON state has been observed for a longer time period until it almost converged to the steady state. Even with a very long ON time of 4.5 s, the slow frequency variation of the VCO is about 16.7 MHz.

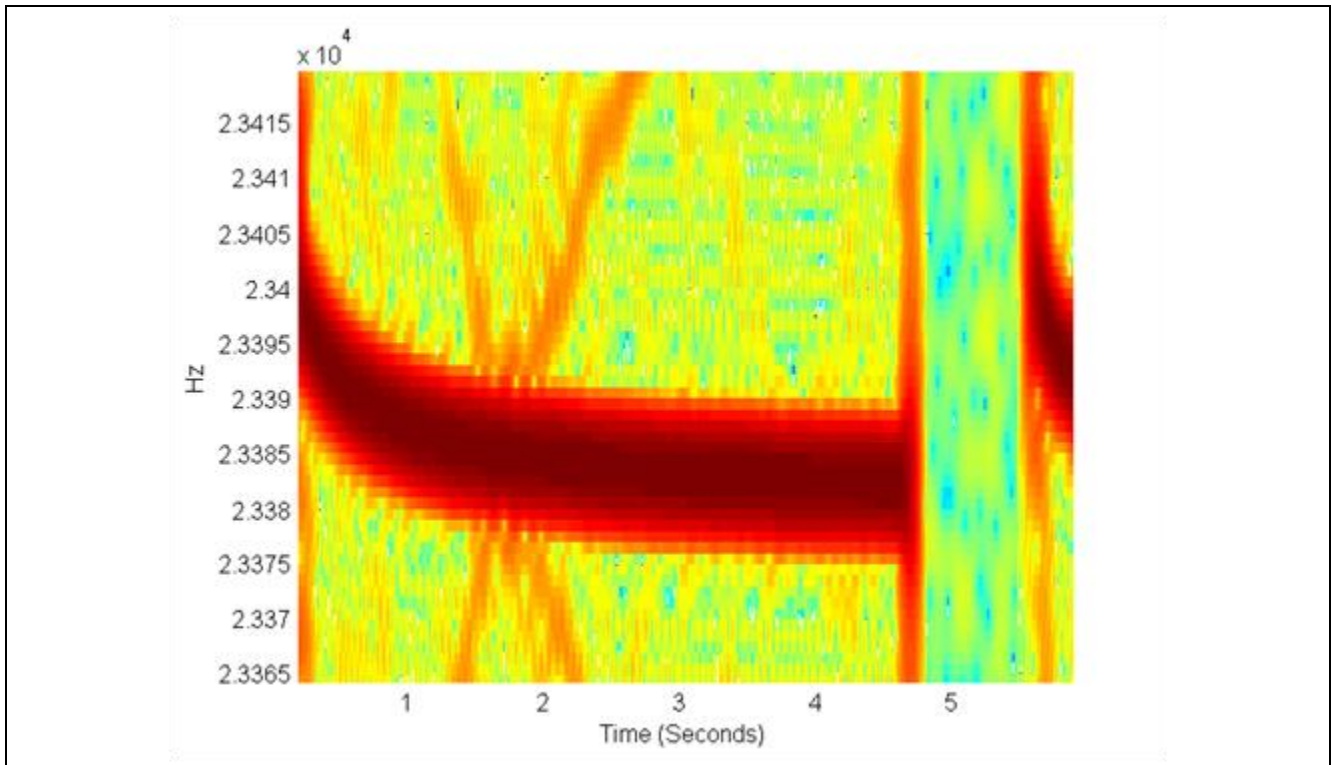


**Figure 17** Spectrogram of oscilloscope data with  $t_{ON} = 4.5$  s and  $t_{OFF} = 1$  s.

Measurements of the temperature sensor output were also conducted. Although distorted by noise as well as by the poor ADC resolution of the used oscilloscope, using a duty-cycle mode with  $t_{ON} = 4.5$  s and  $t_{OFF} = 1$  s, a temperature variation of about 5 °C was measured as shown in Figure 18.

For  $t_{ON} = t_{OFF} = 5$  s, the measured temperature variation through the sensor was about 9 °C to 12 °C.

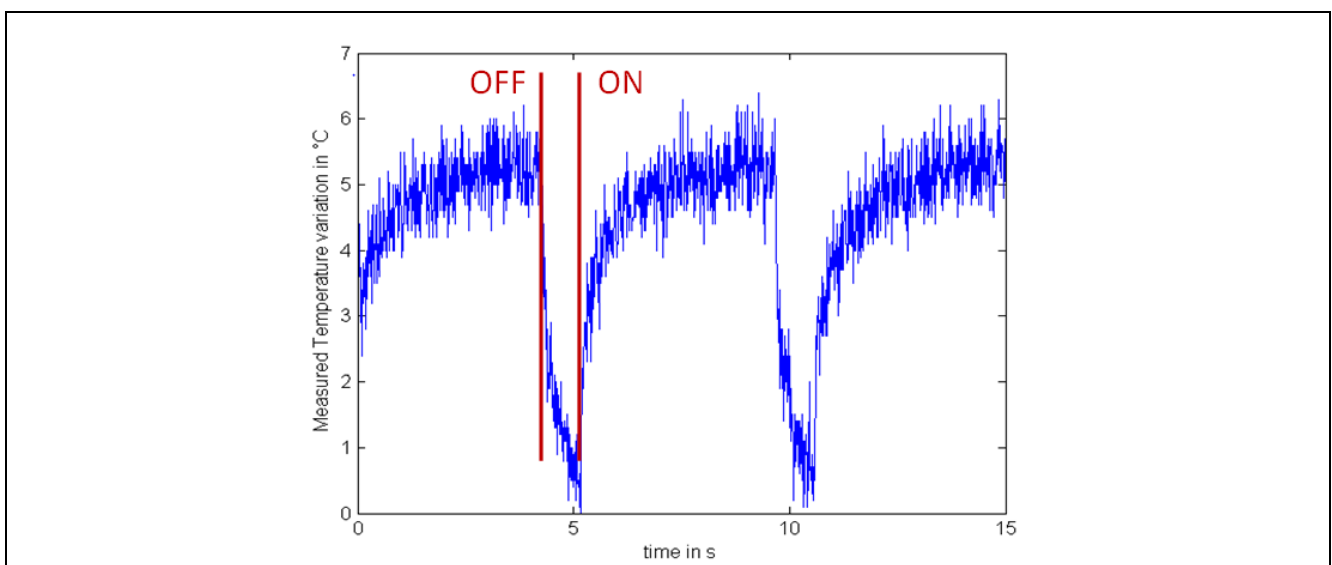


**Figure 18** Temperature variation as a function of time with  $t_{ON} = 4.5$  s and  $t_{OFF} = 1$  s.

It may be concluded from the VCO frequency measurements that:

- A free running VCO radar without a feedback loop to control the frequency is not possible over a large temperature range.
- When the VCO is set to the middle of the ISM band, using the duty-cycle-mode with any duty cycle does not lead to the violation of the ISM band frequency regulation as long as the ambient temperature does not change abruptly.
- In order to account for the ambient temperature variations, the frequency estimation through the 23 kHz prescaler is required before enabling the PA. The frequency may be estimated in a time interval considerably lower than 1 ms.

### 3.2 Sampling time $t_{\text{sample}}$

The sampling time  $t_{\text{sample}}$  is equivalent to the observation time of the Doppler baseband signal contaminated by noise. The target velocity estimation results from the estimation of the Doppler frequency  $f_D$  of the baseband signal described by

$$s_{\text{baseband}}(t) = A \sin(2\pi f_D t) + n(t) \quad (2)$$

with  $A$  the signal amplitude and  $n(t)$  the noise. The velocity measurement is more accurate for a higher value of the signal-to-noise ratio (SNR) of the signal. Accuracy is also increased by having a longer observation time  $t_{\text{sample}}$ . The observation over the limited time  $t_{\text{sample}}$  is equivalent to the multiplication of  $s_{\text{baseband}}(t)$  by a windowing function. In the frequency domain, this is equivalent to a convolution with a sinc pulse  $(\sin(\pi x)/\pi x)$ . The sinc pulse is sharper when the time window is longer. The longer the observation time  $t_{\text{sample}}$ , the more accurate is the estimation. The lowest frequency is the most critical due to its large time period: For 111 Hz  $\rightarrow T \approx 9$  ms.

The SNR may be also improved through a higher sampling frequency over the same time interval  $t_{\text{sample}}$  through the averaging of the high-frequency noise. The sampling rate should also make sure that it is at least equal to the double of the largest Doppler frequency ( $2 \times 888$  Hz  $\approx 1800$  Hz) in order to satisfy the Nyquist sampling theorem.

On the other side, a high sampling rate leads to a larger current consumption and a larger data vector and therefore to much longer digital processing time and required processing resources.

We used in the prototype system a sampling frequency of 5 KSps which lead to acceptable accuracies. The XMC4500 allows a maximum sampling frequency of 2.85 MSps with an 8-bit resolution (uncalibrated).

The SNR is higher for targets closer to the radar, since the reflected signal power is equivalently higher. For a low-power radar operation, it is necessary, given a known SNR, to minimize the observation time without compromising the measurement accuracy beyond the requirements.

Figure 19 shows the statistical simulation of the Doppler Radar system accuracy with SNR = 5 dB and a sampling frequency of 5 KSps and an observation time  $t_{\text{sample}} = 9$  ms. The FFT was used with the factor 5.

The simulation shows that for velocities above 5 km/h, the accuracy remains below the originally specified tolerance of 1 km/h.

It is concluded that the observation time  $t_{\text{sample}} = 9$  ms is sufficient for the targeted radar operation requirements. A higher accuracy or a lower velocity range requires in general a longer observation time.

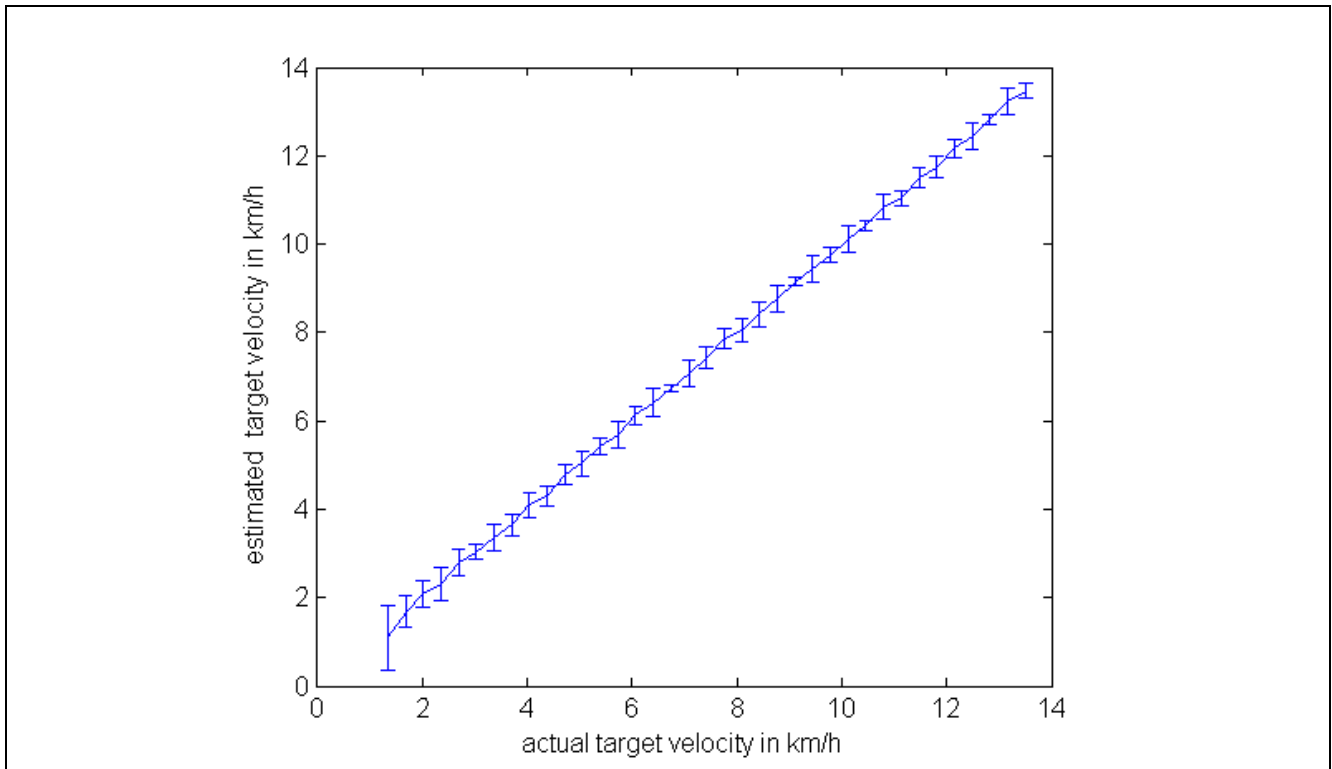


**Figure 19** Simulation of the frequency estimation over the velocity range of interest with SNA = 5 dB,  $f_{\text{sample}} = 5$  KSps and  $t_{\text{sample}} = 9$  ms.

### 3.3 Summary of measurement results

Based on the measurements the VCO settling time  $t_{\text{VCO}}$  may be set to a value lower than 1 ms, which implies that the power ON time of the radar  $t_{\text{ON}}$  is almost equal the sampling time of the ADC. As shown in summarized in Figure 6, the ON time may be set to  $t_{\text{ON}} = 10$  ms, independently from the duty cycle.

By a measurement rate of 2 Hz, the power consumption reduction is equal to a factor of 44. The actual power consumption by a maximal TX power is reduced from about 528 mW to about 11 mW.

The power consumption of the baseband module in the setup was about 48 mW when continuously operated (~ 1 mW in the pulsed mode). The power consumption of the base band module may be further reduced by using more power efficient operational amplifiers.

## 4 Conclusion

This application note shows a way to reduce the overall power consumption of BGT24MTR11 by performing a duty-cycle mode which is also applicable to its siblings BGT24MTR12 and BGT24MR2.

This document gives an estimation on how low one can get in terms of power consumption when turning on and off the radar system – 11 mW compared to above 500 mW in continuous mode. Of course there may be applications that require even lower measurement update rates, for example checking if a parking lot is occupied by a car, resulting in even lower power consumption.

Most other applications will have different needs in terms of sampling time or OFF time, but adjusting those required values one can easily calculate the required duty-cycle, as the switching time can be neglected, to get an estimation of the required power for the radar IC.

## **5       References**

[1] Dietmar Stolz, "User's Guide to BGT24MTR11", AN305, Infineon Technologies AG

[2] Infineon Technologies AG, "XMC4500 Reference Manual", August 2013

## **6       Author**

Dietmar Stolz, Staff Engineer of Business Unit "RF and Protection Devices"



[www.infineon.com](http://www.infineon.com)